Fungal Genetics and Biology 137 (2020) 103349

Contents lists available at ScienceDirect

Fungal Genetics and Biology

journal homepage: www.elsevier.com/locate/yfgbi

MicroRNA-like milR236, regulated by transcription factor MoMsn2, targets histone acetyltransferase MoHat1 to play a role in appressorium formation and virulence of the rice blast fungus *Magnaporthe oryzae*

Ying Li[a], Xinyu Liu[a], Ziyi Yin[a], Yimei You[a], Yibin Zou[a], Muxing Liu[a], Yanglan He[a], Haifeng Zhang[a], Xiaobo Zheng[a], Zhengguang Zhang[a,*], Ping Wang[b]

[a] Department of Plant Pathology, College of Plant Protection, Nanjing Agricultural University, and Key Laboratory of Integrated Management of Crop Diseases and Pests, Ministry of Education, Nanjing 210095, China
[b] Departments of Microbiology, Immunology, and Parasitology, and Pediatrics Louisiana State University Health Sciences Center, New Orleans, LA 70112, USA

ARTICLE INFO

Keywords:
MicroRNA-like RNA
Transcription factor
Appressorium
Virulence

ABSTRACT

MicroRNAs (miRNAs) play important roles in various cellular growth and developmental processes through post-transcriptional gene regulation via mRNA cleavage and degradation and the inhibition of protein translation. To explore if miRNAs play a role in appressoria formation and virulence that are also governed by the regulators of G-protein signaling (RGS) proteins in the rice blast fungus *Magnaporthe oryzae*, we have compared small RNA (sRNA) production between several Δ*Morgs* mutant and the wild-type strains. We have identified sRNA236 as a microRNA-like milR236 that targets the encoding sequence of MoHat1, a histone acetyltransferase type B catalytic subunit involved in appressorium function and virulence. We have also found that milR236 overexpression induces delayed appressorium formation and virulence attenuation, similar to those displayed by the Δ*Mohat1* mutant strain. Moreover, we have shown that the transcription factor MoMsn2 binds to the promoter sequence of milR236 to further suppress *MoHAT1* transcription and MoHat1-regulated appressorium formation and virulence. In summary, by identifying a novel regulatory role of sRNA in the blast fungus, our studies reveal a new paradigm in the multifaceted regulatory pathways that govern the appressorium formation and virulence of *M. oryzae*.

1. Introduction

The RNA interference (RNAi) is a conserved mechanism of gene regulation among primarily eukaryotic organisms that involves small non-coding RNAs (ncRNAs) of 20–40 nucleotides (nt) in length (Lee et al., 2010; Raman et al., 2017). Despite that no specific microRNA (miRNA) was described from the rice blast fungus *Magnaporthe oryzae*, there are numerous components of small RNA (sRNA) repertoire, including small interfering RNA (siRNA) (Kadotani et al., 2003) and methylguanosine-capped and polyadenylated sRNA (CPA-sRNA) found in the fungus (Gowda et al., 2010). There exist putative RNAi pathway components, such as two Dicer-like proteins (MoDcl1 and MoDcl2), three Argonaute proteins (MoAgo1, MoAgo2, and MoAgo3), three RNA-dependent RNA polymerases (MoRdRP1, MoRdRP2, and MoRdRP3), and exportin-5 (Kadotani et al., 2003; Nakayashiki, 2005; Nunes et al., 2011). MoDcl2, MoRdRP2, and MoAgo3 were found to be involved in the biosynthesis of various size classes of sRNAs, while MoRdRP1 and MoAgo3 were involved in fungal virulence (Raman et al., 2017). Studies in *Neurospora crassa* revealed the presence of several new classes of sRNAs, including QDE-2-interacting siRNA (qiRNA), miRNA-like sRNA (milRNA), and Dicer-independent small interfering RNA (disiRNA) (Lee et al., 2010). Based on the evolutional conservation between *M. oryzae* and *N. crassa*, these newer classes of sRNAs are likely to be also present in the blast fungus.

In *M. oryzae*, signal transduction pathways mediated by GTP-binding proteins play important regulatory roles in growth, appressorium formation, and pathogenicity. Accordingly, the regulators of G-protein signaling (RGS) proteins are also important in these regulatory processes (De Vries et al., 2000; Dohlman and Thorner, 2001). We have previously found that *M. oryzae* contains at least 8 RGS and RGS-like proteins with MoRgs1, MoRgs3, MoRgs4, and MoRgs7 all involved in appressorium differentiation and virulence (Zhang et al., 2011b). Since *M. oryzae* contains potentially many sRNA and miRNA classes, we hypothesize that they may exhibit regulatory roles over RGS proteins

* Corresponding author.
E-mail address: zhgzhang@njau.edu.cn (Z. Zhang).

https://doi.org/10.1016/j.fgb.2020.103349
Received 9 January 2020; Accepted 28 January 2020
Available online 29 January 2020

governing appressorium formation and virulence.

By profiling the production of sRNAs through sRNA-Seq of the Δ*Morgs1*, Δ*Morgs3*, and Δ*Morgs7* mutants, as well as wild-type Guy11 during the initial stage of appressorium formation, we have identified 219 milRNAs and 171 non-redundant differentially expressed milRNAs (DE-milRNAs). Among them, milR236 was found to target the gene sequence of *MoHAT1* encoding the histone acetyltransferase type B catalytic subunit. The overexpression of milR236 resulted in delayed appressorium formation and attenuated virulence, which were similar to those displayed by the Δ*Mohat1* mutant strain. Intriguingly, we also found that milR236 is subjected to transcriptional regulation by the transcription factor MoMsn2.

2. Materials and methods

2.1. Fungal strains and RNA samples

M. oryzae strain Guy11 was used as the wild type, and Δ*Morgs1*, Δ*Morgs3*, Δ*Morgs7,* and Δ*Momsn2* were described previously (Zhang et al., 2014, 2011b). Conidia of Guy11, Δ*Morgs1*, Δ*Morgs3*, and Δ*Morgs7* were respectively harvested from 10-day-old SDC agar cultures, filtered through three layers of lens paper, and resuspended to a concentration of 10^5 spores/ml. Droplets (200 μl) of conidial suspension were placed on the GelBond® film (Lonza Rockland, ME USA) under humid conditions at 28 °C for 4 h. Liquid supernatants were discarded and the appressoria were collected for RNA extraction, library construction, and qRT-PCR analysis. Two additional experiments under the same condition were carried out to serve as biological replicates.

2.2. Small RNA isolation, library construction, and sequencing

Total RNA was isolated using the Trizol reagent (Invitrogen, New York). The RIN (the RNA integrity number) of all samples was > 8.0. The library construction of 16 small RNAs (4 strains each with 3 biological duplications) and Illumina sequencing were completed by Beijing Genomics Institute (BGI), Shenzhen, China. The reads of sRNAs over 16 nt were mapped to the *M. oryzae* Guy11 genomes and annotated (Zhang et al., 2013).

2.3. sRNA analysis by RT-PCR and Northern hybridization

Following Trizol extraction, RNA was treated with DNase prior to reverse transcription. cDNA synthesis and RT-PCR were the same as described previously (Dong et al., 2015). Briefly, reverse transcription was carried out in a reaction with 4 μl of 5 × HiScriptII qRT super MixII and specific RT primer mixes (Varkonyi-Gasic et al., 2007). The reaction was incubated at 50 °C for 15 min and deactivated at 85 °C for 5 s. The stem-loop RT-PCR was performed by the SYBR green master mix to detect the abundance of milRNAs (Dong et al., 2015; Varkonyi-Gasic et al., 2007). Primers used for reverse transcription and real-time PCR amplification were listed in Table S5.

Northern blot analysis of milRNA was performed following the protocols described previously (Hu and Zhu, 2017; Huang et al., 2014). Briefly, sRNAs (10 μg) were isolated from total RNA by precipitation in 5% PEG8000 and 0.5 M NaCl. sRNAs were resolved using 14% denaturing polyacrylamide gel electrophoresis, transferred to the nylon membrane (GE healthcare life sciences), and detected by the biotin-labeling method (NEB). Quantitation of the blots was performed using ImageJ and the relative signals were calculated by normalizing to the *Actin* gene control. Probes used for RNA blotting analysis were listed in Table S5.

2.4. Retrieval of promoter sequences

One kb upstream sequences were retrieved at the beginning of the pre-miRNA for the prediction of TSS (Transcription Start Site), which were the putative promoter sequences. It is considered that miRNA may be located inside the encoding sequence, 5′ untranslated region (UTR), or 3′ UTR, but the promoter sequence may remain the same. The putative promoter sequence was used for motif search.

2.5. Electrophoretic mobility shift assay (EMSA) analysis

The full-length DNA of the promoter of milR236 was amplified from Guy11 genomic DNA using primers milR236-Pro-F/milR236-Pro-R (Table S5). The DNA fragment from the milR236 promoter was end-labeled with Alex660 by PCR amplification using the 5′-Alex660-labelled primer. The MoMsn2 protein was expressed and purified from *Escherichia coli* strain BL21 using the pET32a construct containing 6xHis-tag coding sequence. The purified protein (50 μg) was mixed with Alex660-labelled DNA (2 μg), incubated for 20 min at 25 °C in binding buffer and separated by agarose gel electrophoresis. Gels were visualized directly using a LI-COR (Lincoln, NE, USA) Odyssey scanner with excitation at 700 nm (Wang et al., 2017).

2.6. milR236 overexpression

We generated a milR236-overexpression (milR236-OE) vector based on the method previously described (Schwab et al., 2006). First, the mature sequence of milR236 was uploaded into WMD3 (http://wmd3.weigelworld.org) and the RS300 vector was selected and four primer sequences determined. The generation of functional milRNA precursors was achieved by overlap PCR. The PCR products were ligated into the pYF11 vector containing the ribosomal protein 27 gene promoter.

2.7. Appressorium formation and function and virulence assays

To assess appressorium formation, droplets (30 μl) of conidial suspension were placed on plastic coverslips (Fisher Scientific, USA) under humid conditions at 28 °C (Zhang et al., 2011a). The appressorium turgor was determined by cell collapse assay using a 1–4 M concentration of glycerol solution. The percentages of conidia germinating and conidia forming appressoria were determined by microscopic examination of at least 100 conidia.

Conidia were harvested from 10-day-old SDC agar cultures, filtered through three layers of lens paper, and resuspended to a concentration of 5 × 10^4 spores/ml in a 0.2% (wt/vol) gelatin solution. For the leaf assay, leaves from two-week-old seedlings of rice (*Oryza sativa* cv. CO39) were used for spray inoculation. Spray inoculation and pathogenicity assays performed according to Zhang et al. (2011a).

For infection assay with rice tissues, 3-week-old rice cultivar CO39 was inoculated with 100 μl conidial suspension (1 × 10^5 spores/ml in a 0.2% (w/v) gelatin solution) on the inner leaf sheath cuticle cells and incubation under humid conditions at 28 °C. The leaf sheaths were observed under Zeiss Axio Observer A1 inverted microscope at 48 hpi.

2.8. In vitro protein purification

To construct *MoMSN2:His* vectors, full-length *MoMSN2* cDNA was first amplified and inserted into the vector pET-32a. The plasmids were expressed in *E. coli* strain BL21 and bacterial cells were collected and treated by lysis buffer (10 mM Tris-HCl [pH 7.5], 150 mM NaCl, 0.5 mM EDTA, 0.5% Triton x-100). For MoMsn2:His, the bacterial lysate was incubated with 30 μl Ni-NTA agarose beads (Invitrogen, Shanghai, China) at 4 °C and then the beads were washed for five times. The eluant was reduced with Glutathione (Abmart, Shanghai, China). Coomassie blue staining of the MoMsn2:His protein was shown in Supplementary Fig. S6.

2.9. Agrobacterium-mediated transient expression assay in Nicotiana benthamiana

The binary vector pBIN:GFP4 was used for to express the milRNA target gene *MoHAT1* and target-mutant gene *MoHAT1*^{DTB} in which a synonymous mutation occurs when the binding sequence "GAC CTC CGT ATC AAT ACA GAC" is changed to "GAT CTT AGA ATA AAC ACC GAT". MiRNA was cloned into the milR236 backbone vector (Schwab et al., 2006) and transferred into the binary vector pBIN:HA for expression. Following co-expression of milRNA and its target gene about 36 h, leaves were examined and images were acquired using an Axio Observer A1 Zeiss inverted microscope as previously described (Li et al., 2017). Protein products of the target genes were also examined by Western blot analysis.

3. Results

3.1. Morgs mutant strains display dynamic sRNA expression patterns during appressorium formation

Previous studies have demonstrated that RGS proteins MoRgs1, MoRgs3, MoRgs4, and MoRgs7 are all involved in appressorium differentiation and the virulence of *M. oryzae* (Zhang et al., 2011b). To explore whether the function involves sRNA regulation, we performed sRNA-Seq for Guy11, Δ*Morgs1*, Δ*Morgs3*, and Δ*Morgs7* strains at 4 h post-inoculation (hpi) on the artificial inductive surface that corresponds to the appressorium development stage. Since the conidium production of Δ*Morgs4* mutant was severely impaired (Zhang et al., 2011b), the Δ*Morgs4* mutant was not used in the sRNA-Seq study.

sRNA libraries were generated and subjected to deep sequencing following quality assessment. Approximately 19.6 million clean reads were obtained from the Guy11, Δ*Morgs1*, and Δ*Morgs7* strains, and 18.8 million clean reads were obtained from the Δ*Morgs3* strain. Of these reads, 69.79 (Guy11), 77.28 (Δ*Morgs1*), 56.57 (Δ*Morgs3*), and 63.40% (Δ*Morgs7*) were mapped to the *M. oryzae* genome (Table 1). These reads were further matched to intergenic regions, exons and introns of coding sequences, precursors, small nuclear RNA (snRNA), small nucleolar RNA (snoRNA), ribosomal RNA (rRNA), and transfer RNA (tRNA). The size distribution of the total genome-matched reads showed the peaks of from 19 to 23 nt (Supplementary Fig. S1). Analysis of the 5′ nucleotide preferences of sRNA (18–30 nt) from the libraries of various Δ*Morgs* mutants revealed that sRNAs starting with U were the most abundant (Supplementary Fig. S2).

In contrast to plants and animals, no conventional miRNAs has been reported in filamentous fungi. Instead, many miRNA-like (milRNA) sequences, which are produced by similar but not identical mechanisms as those for conventional miRNAs, were found in *N. crassa* (Lee et al., 2010; Ruby et al., 2006) and *Verticillium dahliae* (Jin et al., 2019). Using the criteria of animal and plant miRNAs, such as the ability to form hairpin structures with flanking sequences and the most abundant sRNA species residing in the stem region of the hairpin structure, 219 novel milRNAs were predicted by Mireap software (https://sourceforge.net/projects/mireap/) described by Li et al. (2012) that were presumably related to appressorium formation (Table S1). By comparing the expression levels of milRNAs in the three Δ*Morgs* mutants against those in Guy11, we also identified 171 non-redundant differentially expressed (DE)-milRNAs (Fig. 1A and Supplementary Table S2). In addition, most of the DE-milRNAs appeared to be specific to RGS proteins, as no consensus pattern was observed. We further selected several random up- and down-regulated milRNAs and validated their expression by qRT-PCR. The results indicated that the expression levels for one out of five (milR028) in Δ*Morgs1*, five out of ten (milR204, milR070, milR048, milR062, and milR036) in Δ*Morgs3*, and five out of seven (milR104, milR197, milR221, milR027, and milR166) in Δ*Morgs7* were generally in agreement with the results of sRNA-Seq (Supplementary Fig. S3). These findings indicated that there was a consistency between the two approaches.

3.2. DE-milRNAs are regulated by the transcription factor MoMsn2

miRNA precursors (pre-miRNAs) derived from primary transcripts (pri-miRNAs) are primarily regulated by transcription factors (TFs) (Guo et al., 2010; Hackenberg et al., 2012). To test potential TFs that regulate milRNAs, we analyzed the promoter sequences (~1.0 kb) of 171 DE-milRNAs using the MEME program (http://meme-suite.org/tools/meme). We found that 70.76% of the sequences share a common motif (Fig. 1B and Supplementary Table S3) that is highly homologous to that of the *MSN2* gene in *Saccharomyces cerevisiae* (http://jaspar.genereg.net) (Fig. 1C). In *M. oryzae*, MoMsn2 is the ortholog of ScMsn2 (Zhang et al., 2014). We then assessed the expression of *MoMSN2* at an early stage of appressorium formation in the Δ*Morgs1*, Δ*Morgs3*, Δ*Morgs7* mutant strains and Guy11 using qRT-PCR. The results confirmed that the expression of *MoMSN2* was significantly reduced in these mutants (Fig. 1D). To further examine how MoMsn2 regulates milR083, milR293, milR027, and milR062, qRT-PCR was again performed that showed they were significantly downregulated in the Δ*Momsn2* mutant (Fig. 1E). Moreover, promoter sequence binding by MoMsn2 was carried out using the electrophoretic mobility shift assay (EMSA) that showed the promoter sequence was retarded by the addition of the purified MoMsn2 protein but not the mutant promoter sequence lacking the binding motif (Fig. 1F). The addition of proteinase K diminished this binding (Fig. 1F). This result indicated that MoMsn2 regulates the expression of DE-milRNAs by binding to their promoter sequences.

3.3. Co-regulated DE-milRNAs and candidate target genes

Target gene identification was carried out using TargetFinder and psRobot. Among 12 co-regulated DE-milRNAs, 5 (milR015, milR064, milR136, milR170, and milR196) had no target genes identifiable while the remaining seven milRNAs had predicted targets. The expression of these seven DE-milRNAs (precursors) in Δ*Morgs1*, Δ*Morgs3*, Δ*Morgs7*,

Table 1
Distribution of small RNAs among different categories in each library.

Type/Reads	Guy11	Δ*Morgs1*	Δ*Morgs3*	Δ*Morgs7*
Total reads	19,591,019	19,588,815	18,809,892	19,624,084
Mapped genome reads	13661532(69.79%)	15137042(77.28%)	10648422(56.57%)	12444076(63.40%)
intergenic region	3,033,839	3,528,741	2,024,489	4,695,961
intron	75,961	107,196	45,314	88,586
exon	1,422,326	2,276,379	758,068	1,277,542
precursor	1455	1479	1306	1579
sRNA	62,992	74,903	28,983	34,257
snRNA	1608	2795	1009	1031
snoRNA	7920	10,621	4123	6697
rRNA	586,087	470,704	365,012	347,977
tRNA	14,863	17,246	6079	7817

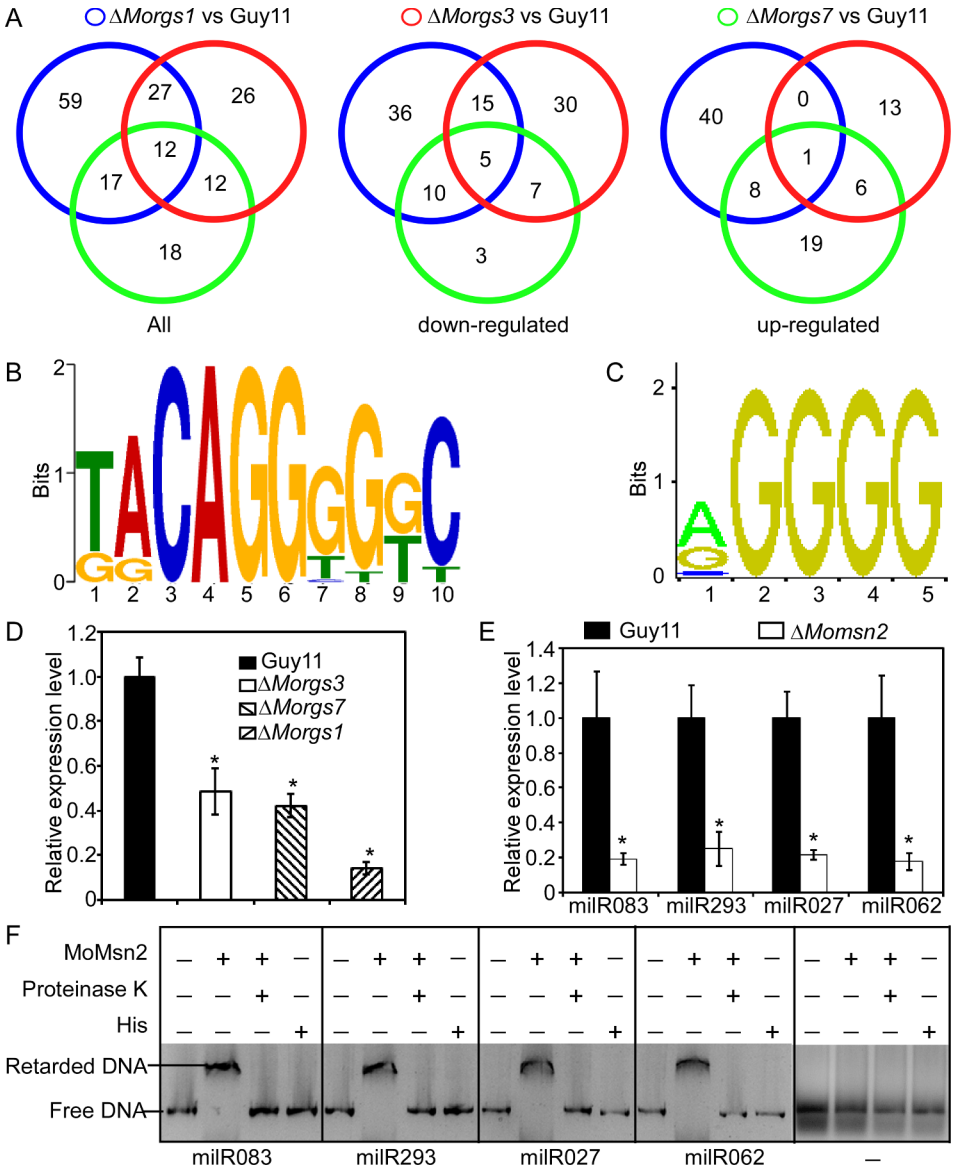

Fig. 1. Differentially expressed milRNAs are regulated by the transcription factor MoMsn2. (A) Venn analysis of Δ*Morgs1*, Δ*Morgs3*, and Δ*Morgs7* in comparison to Guy11 revealed that 12 milRNAs are commonly shared. The differentially expressed milRNAs in three mutants were clustered by Venn analysis. (B) DNA motifs were generated by MEME from promoter analysis of 121 differentially expressed milRNAs. (C) The putative binding motif of Msn2 identified in the JASPAR database. (D) The expression of *MoMSN2* was down-regulated in the Δ*Morgs1*, Δ*Morgs3*, and Δ*Morgs7* strains at 4 h after infection. Error bars represent standard deviation; asterisks represent significant differences between the strains ($P < 0.01$) based on Duncan's new multiple range test. (E) The expression of milR083, milR293, milR027, milR062 were down-regulated in Δ*Momsn2*. Error bars represent standard deviations; asterisks denote statistical significance ($P < 0.01$) based on the Student's *t* test. (F) Validation of MoMsn2 binding to promoters of milRNAs by EMSA. The full-length DNA of the promoters of milR083, milR293, milR027, and milR062 was incubated in the absence (first lane) or presence of purified MoMsn2 (second lane) and His protein (fourth lane). Proteinase K was added after the incubation of MoMsn2 with DNA (third lane). DNA–protein complexes were separated by electrophoresis on a 1.5% agarose gel. (The first lane with the full-length DNA of the milRNA promoters, as control; the second lane: the full-length promoter DNA was incubated with purified MoMsn2; the third lane: Proteinase K was added after MoMsn2- DNA incubation; and the fourth lane: the incubation of the His protein with DNA, as control.) The last column was the negative control with no binding sequence.

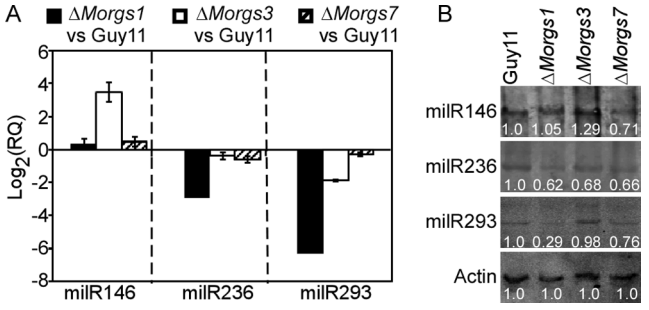

Fig. 2. Co-regulated milRNAs were validated by qRT-PCR and Northern blot analysis. (A) Quantitative real-time PCR (qRT-PCR) expression analysis of milR146, milR236, and milR293 in the Δ*Morgs1*, Δ*Morgs3*, and Δ*Morgs7* mutant strains in contrast to wild-type Guy11. (B) Northern blot analysis of three milRNAs. Expression was normalized to the transcript of the actin gene and the relative value was inserted in the picture beneath the milRNA band. The experiments were repeated twice that showed similar results.

and Guy11 was examined by qRT-PCR (Table S4). The expression of milR146 was upregulated, while the expression of milR236 and milR293 was down, in all three mutants (Fig. 2A). By using reverse-complementary DNA fragments as the probes (Table S5), we performed Northern blot analysis to validate these results. The mature sequences of milR146, milR236, and milR293 all have a length of 20 nt. The expression of milR146 showed discernible upregulation in Δ*Morgs3,* downregulation in Δ*Morgs4*, and no obvious changes in Δ*Morgs1*, whereas milR236 and milR293 showed significant reduced expression in all three mutants (Fig. 2B). The expression levels of milR236 were consistent with the qRT-PCR data, whereas the expression of milR146 and milR293 showed a slight inconsistency (Fig. 2B).

miRNAs target the mRNA of target genes for degradation, thereby suppressing gene expression (He and Hannon, 2004). We analyzed the expression of candidate target genes of the three milRNAs in the Δ*Morgs* mutants using qRT-PCR (Table S6 and Fig. 3). We found that milR146 significantly suppressed the expression of MGG_07848, and the suppression was validated using a milR146 overexpression strain (milR146OE) (Supplementary Fig. S4A). The expression of MGG_06375 was upregulated in Δ*Morgs1*, Δ*Morgs3*, and Δ*Morgs7*, which contain the shortened versions of milR236, as compared with that of Guy11. Meanwhile, of all the candidate targets of milR293, only MGG_17707 showed upregulated expression in the three Δ*Morgs* mutants (Fig. 3).

We selected these three target genes for further characterization by generating knockout mutants. We were able to obtain mutant strains of

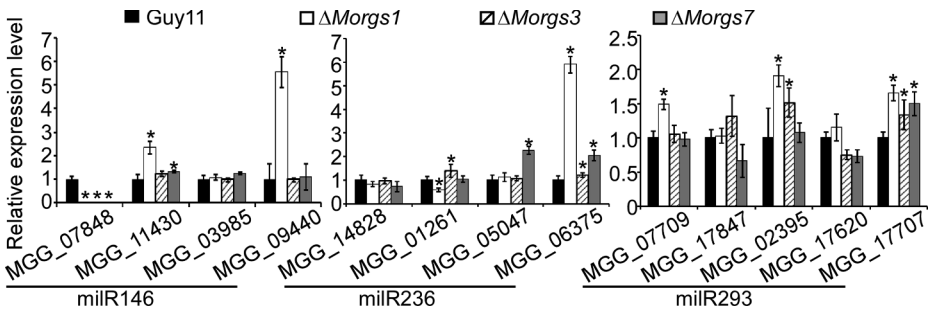

Fig. 3. The candidate target genes were validated by qRT-PCR. Expression analysis of candidate target genes of milR146, milR236, and milR293 in Guy11 wild-type, Δ*Morgs1*, Δ*Morgs3*, and Δ*Morgs7* mutant strains. The experiments were repeated twice that showed similar results. Error bars represent the standard deviation and asterisks represent significant differences (Duncan's new multiple range tests, $P < 0.01$).

MGG_07848 and MGG_06375 but not MGG_17707. Since the MGG_07848 mutant exhibited no detectable phenotypic change (Supplementary Fig. S4B), we placed the focus on MGG_06375 and found that it encodes a *M. oryzae* homolog of the histone acetyltransferase type B catalytic subunit Hat1 in *S. cerevisiae*. We thus named MGG_06375 gene product as MoHat1.

In *S. cerevisiae*, histone H3 and Hat1 contribute to DNA double-strand break repair, and a *Schat1* null mutant was sensitive to the DNA-damaging agent methyl methanesulfonate (MMS) (Qin and Parthun, 2002). We have recently demonstrated that the expression of MoHat1 partially rescued the sensitivity defect to MMS in *Schat1* and MoHat1 has a function in appressorium development and pathogenicity of *M. oryzae* (Yin et al., 2019).

3.4. milR236 is regulated by the transcription factor MoMsn2

To test the genetic relationship between milR236 and MoHat1, we examined whether MoMsn2 binds to the milR236 promoter. First, we mapped the milR236 precursor to the 3′ untranslated region of MGG_09408 encoding a cyclic nucleotide-binding domain-containing protein, indicating milR236 shares a promoter with MGG_09408. To determine whether this promoter functions in the expression of milR236, we fused it with the green fluorescent protein (GFP) to construct Pro-milR236:GFP. As a positive control, we also fused GFP to the constructively activated rp27 promoter (rp27:GFP). Under the same conditions, rp27:GFP fluorescence was stronger than that of the strain expressing Pro-milR236:GFP (Supplementary Fig. S5A). Western blot analysis indicated that the expression of GFP in the rp27:GFP strain was also stronger than that of Pro-milR236:GFP (Supplementary Fig. S5B). These results suggested that milR236 is subjected to regulation by the MGG_09408 promoter.

Within the promoter sequence, we further identified a putative binding motif by the transcription factor MoMsn2. We first verified that the expression of milR236 is downregulated in the Δ*Momsn2* mutant (Fig. 4A), and then performed EMSA to test the binding between MoMsn2 and the promoter of milR236. Results showed that DNA containing the promoter sequence was retarded by the addition of the purified MoMsn2 protein, and this retardation was significantly increased as the amount of MoMsn2 was increased (Fig. 4B, C) and diminished when proteinase K was added (Fig. 4B). Competition binding revealed that, with increasing concentrations of 1-, 2-, 5-, or 10-fold excess of unlabeled competitor DNA, the retardation of Alexa Fluor 660-labeled 1000-bp DNA was weakened (Fig. 4D). Taken together, these results demonstrated that MoMsn2 binds to the promoter of milR236 to further regulate the expression of milR236.

3.5. milR236 downregulates the expression of MoHAT1

As miRNAs play a role in suppressing the expression of target genes, we hypothesized that the target genes could be suppressed during the growth and development of *M. oryzae*. Therefore, we examined the expression of milR236 and *MoHAT1* at different stages of development, including mycelium (MY), conidium (CO), and appressorium formation

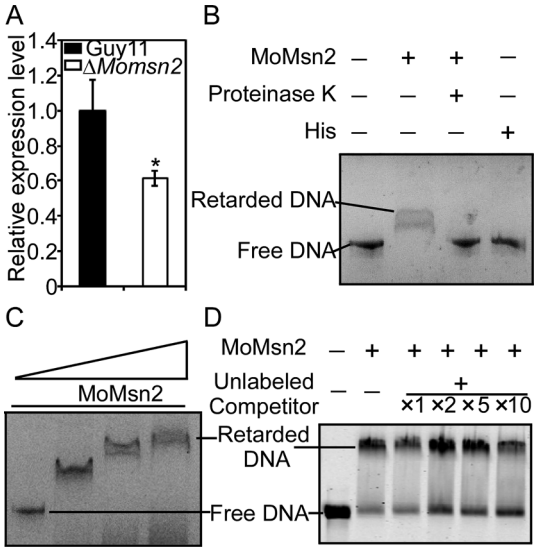

Fig. 4. milR236 was regulated by MoMsn2. **(**A) The expression of milR236 was down-regulated in Δ*Momsn2*. Error bars represent standard deviation; asterisks denote statistical significance ($P < 0.01$) based on the Student's *t* test. (B) The full-length promoter sequence of milR236 was incubated in the absence (first lane) or presence of purified MoMsn2 (second lane), and the His protein (fourth lane). Proteinase K was added after the incubation (third lane). DNA–protein complexes were separated by electrophoresis on a 1.5% agarose gel. DNA was retarded by the addition of MoMsn2. (C) Increasing amounts of MoMsn2 (50 μg, 100 μg, 150 μg) were incubated with 1000-bp DNA (2 μg). The complexes were resolved by electrophoresis on a 1.5% agarose gel. The DNA band was retarded significantly with the increasing amount of MoMsn2. (D) MoMsn2 (50 μg) was incubated with Alex660-labelled 1000-bp DNA in the absence or presence of 1-, 2-, 5-, or 10- excess of the corresponding unlabeled competitor DNA and analyzed by electrophoresis. The experiment was repeated three times with similar results.

(AP-4 hpi) in the Δ*Morgs1* strain by qRT-PCR (Fig. 5A, B). As anticipated, the expression of milR236 was lower than that in Guy11 and the lowest level was at the appressorium formation stage (4 hpi). In contrast, the transcripts of *MoHAT1* were abundant, particularly at 4 hpi, the presumed appressorium formation stage. To further understand that milR236 regulates the function of its target, we transduced the milR236 into the Δ*Mohat1:MoHAT*^{DTB} and Δ*Mohat1:MoHAT* to obtain the Δ*Mohat1:MoHAT*^{DTB}*:milR236* (H^D-M) and Δ*Mohat1:MoHAT:milR236* (H-M-1 and H-M-6) strains. We first verified that the levels of milR236 were all up-regulated in these strains (Fig. 5C). We then observed that the expression of *MoHAT1* was reduced in the Δ*Mohat1:MoHAT:milR236* strain but not the Δ*Mohat1:MoHAT*^{DTB}*:milR236* strain (Fig. 5D). We also tested the expression of *MoHAT1* in H^D-M and H-M-1 at various stages of development (MY, CO, AP-2 h, AP-4 h) in comparison to the control (Fig. 5E) and the results were consistent with that milR236 suppresses the expression of *MoHAT1*. Moreover, we detected the protein levels (AP-4 h) of MoHat1^{DTB} and MoHat1 with milR236 by Western blotting analysis that showed a 3.5-fold reduction in the accumulation of the

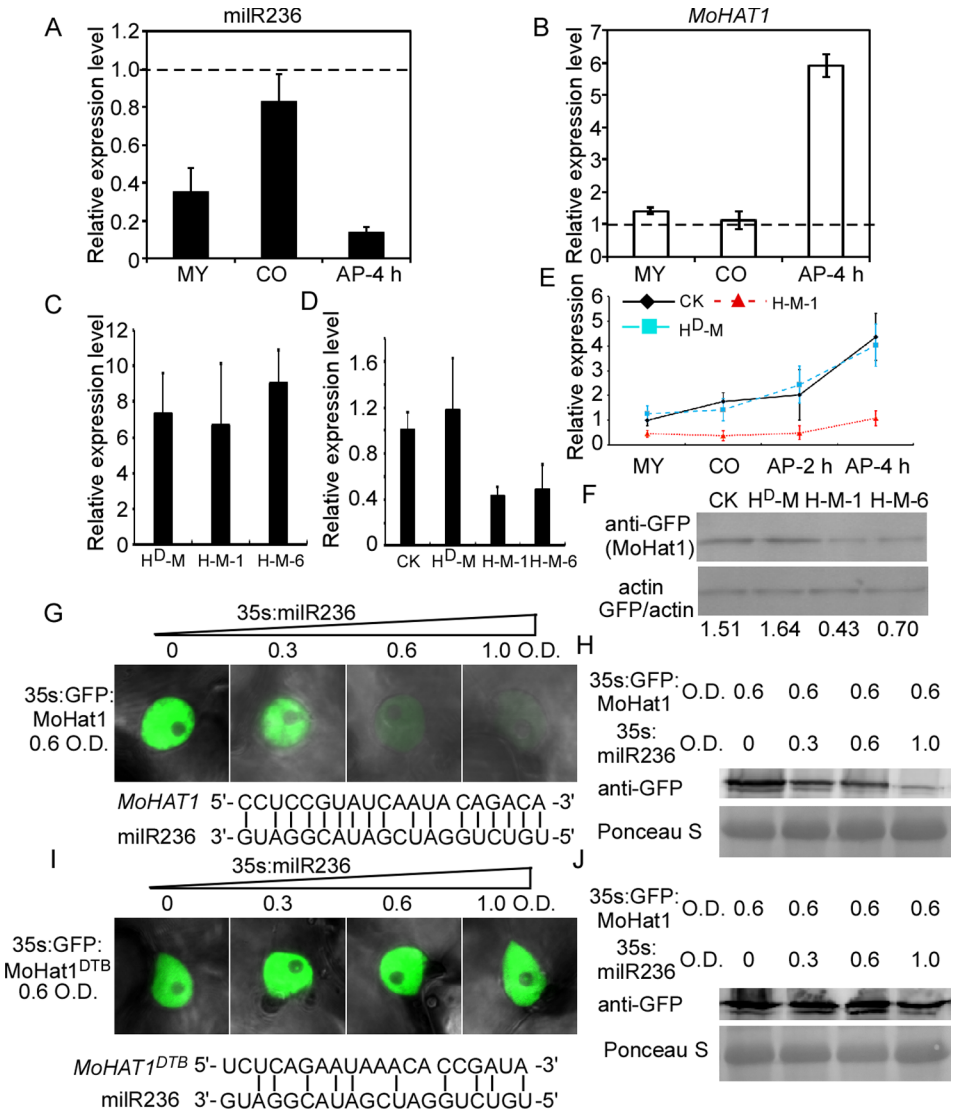

Fig. 5. milR236 down-regulates the expression of *MoHAT1* at the transcriptional level. (A) The expression of milR236 at different stages of the Δ*Morgs1* mutant strain. MY: mycelium, CO: conidium, AP-4 h: appressorium formation 4 h. The dotted line represents the expression of milR236 at different stages of the Guy11 strain. (B) Relative mRNA levels of *MoHAT1* in different stages of the Δ*Morgs1* mutant strain. The expression of milR236 was lower, while the expression of *MoHAT1* was higher. The dotted line represents the expression of *MoHAT1* at different stages of the Guy11 strain. The experiment was repeated three times with the same results. (C) Transcription levels of milR236 were assayed in the Δ*Mohat1:MoHAT*^{DTB}*:milR236* (H^D-M) and Δ*Mohat1:MoHAT:milR236* (H-M-1 and H-M-6) strains. milR236 in all these strains were up-regulated. (D) Expression of *MoHAT1* and *MoHAT1*^{DTB} in the Δ*Mohat1:MoHAT*^{DTB}*:milR236* (H^D-M) and Δ*Mohat1:MoHAT:milR236* (H-M-1 and H-M-6) strains. (E) Expression of *MoHAT1* in the H^D-M, H-M-1 and CK (Δ*Mohat1:MoHAT*) strains at different stages (MY, CO, AP-2 h, AP-4 h). (F) Western blotting analysis (AP-4 h) showed that the accumulation of MoHat1-GFP proteins in the Δ*Mohat1:MoHAT*^{DTB}*:milR236* (H^D-M) and Δ*Mohat1:MoHAT:milR236* (H-M-1 and H-M-6) strains. MoHat1 and MoHat1^{DTB} proteins were detected with the GFP antibody and actin was used as control. (G-J) Confocal images and Western blotting analysis showed that milR236 suppresses the protein accumulation of MoHat1 by targeting the coding sequence. (G/H) GFP:MoHat1 was transiently expressed alone or co-expressed with milR236 or (I/J) target mutant GFP:MoHat1^{DTB} was transiently expressed alone or co-expressed with milR236 in *N. benthamiana* leaves using *Agrobacterium*-mediated infiltration at the indicated optical density (O.D.) concentration. (G) and (I) was recorded by observing at least 50 cells for each treatment and the experiment was repeated three times. Protein extracts from the same amount of infiltrated leaves were subjected to Western blot analysis using the anti-GFP antibody. The Coomassie Blue stained Rubisco indicated an equal sample loading. Similar results were obtained in at least two independent experiments.

MoHat1 protein (H-M-1). However, no reduction in the MoHat1^{DTB} protein (H^D-M) was found that was consistent with the levels of transcripts (Fig. 5F).

We then generated the pBin:GFP:MoHat1 construct to test whether milR236 inhibits the protein expression. To do this, GFP:MoHat1 was separately expressed or co-expressed with milR236 in the plant *Nicotiana benthamiana* and protein levels were analyzed by Western blotting and GFP fluorescence estimation. The results showed that GFP:MoHat1 was highly expressed and accumulated in the nucleus when expressed alone (Fig. 5G). However, this expression level was reduced when co-expressed with milR236, particularly at higher optical densities of infiltrated *Agrobacteria* (Fig. 5H). Moreover, GFP:MoHat1^{DTB}, which has a synonymous mutation at the target sequences leading to mismatch, was also co-expressed with milR236, and the accumulation of GFP:MoHat1^{DTB} protein did not change following the addition of milR236, as indicated by Western blotting and fluorescence estimation (Fig. 5I, J). These results indicated that the suppression of GFP:MoHat1 by milR236 was rescued by the synonymous mutation of the target sequence.

3.6. milR236 overexpression reduces virulence and delays appressorium formation

In *M. oryzae*, MoHat1 plays an important role in appressorium formation and virulence (Yin et al., 2019; Zhang et al., 2017). Since milR236 suppresses the expression of MoHat1 and its expression was at the lowest level in the Δ*Morgs1* mutant, we hypothesize that milR236 also functions in appressorium formation and virulence. First, we generated a milR236-overexpression (milR236-OE) strain and observed that the expression of milR236 was more than five times higher than that in Guy11 (Fig. 6A). And the Northern blot confirmed the mature of milR236 in the milR236-OE strain was 1.5 times greater than that in Guy11 at the expected length (20 nt) (Fig. 6B). In addition, virulence testing showed that the milR236-OE strain caused fewer, but restricted, lesions on the susceptible (CO39) rice seedling leaves, similar to that caused by the Δ*Mohat1* mutant (Fig. 6C, D). However, when the MoHAT1^{DTB} was introduced to the milR236-OE strain, virulence was returned to the wild-type level (Fig. 6C, D). We also tested the virulence of Δ*Mohat1*:MoHAT1^{DTB} strain as the control, and found that the

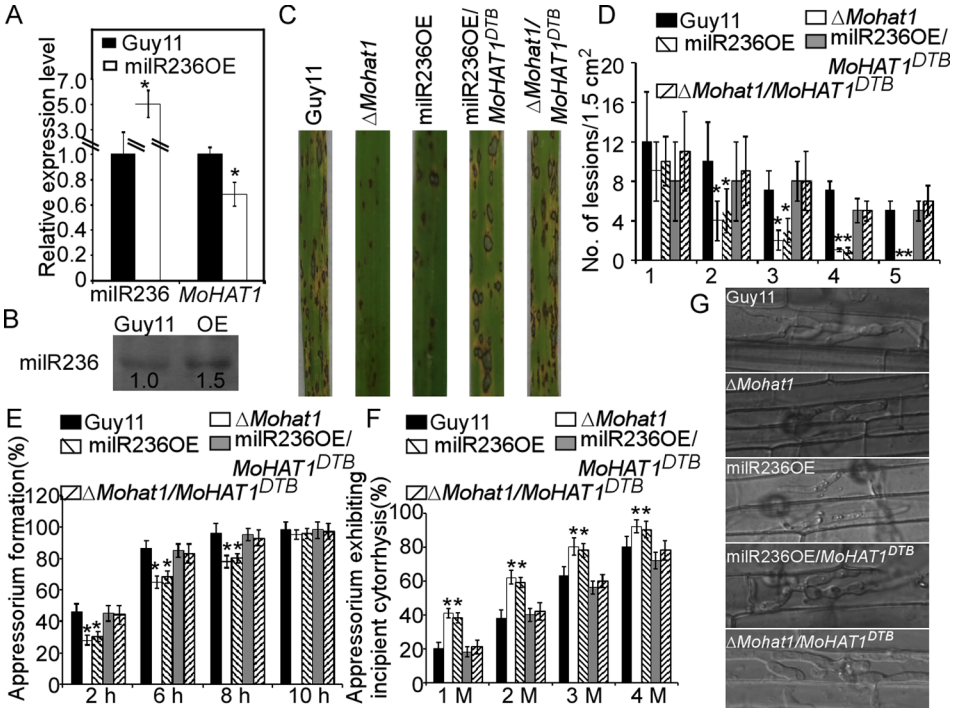

Fig. 6. milR236 overexpression results in delayed appressorium formation and virulence attenuation. (A) Expression detection of milR236 and *MoHAT1* in the overexpression strain by qRT-PCR. Error bars represent the standard deviation and asterisks represent significant differences (Student's *t* test, $P < 0.01$). (B) Northern blot analysis of milR236 in Guy11 and milR236-OE strains. (C) Disease symptoms were reduced on rice leaves spray inoculated with the Δ*Mohat1*, milR236OE, milR236OE/MoHAT1^{DTB} , Δ*Mohat1*:MoHAT1^{DTB}s trains. Three independent experiments were performed. (D) Quantification of lesion types. Lesions were photographed and scored at 7 days post-inoculation (dpi) and experiments were repeated three times with similar results. Numbers within an area of 1.5 cm^2 of 20 rice leaves infected by each strain were counted. Asterisks represent significant differences (Duncan's new multiple range test, $P < 0.01$). (E) Appressorium formation rates at different time-points were calculated and statistically analyzed. The percentage at a given time was recorded by observing at least 100 conidia for each strain and the experiment was repeated three times. Error bars represent standard deviation and asterisks represent significant difference (Duncan's new multiple range test, $P < 0.01$). (F) Appressorium turgor was measured by an incipient cytolysis (cell collapse) assay in the presence of 1, 2, 3 and 4 M glycerol. The percentage of collapsed appressoria was recorded by observing at least 100 appressoria and the experiment was repeated three times. Error bars represent standard deviation and asterisks represent significant difference (Duncan's new multiple range test, $P < 0.01$). (G) Penetration assays in rice sheath. IH growth on rice cells was observed at 48 hpi and the main type of IH was quantified and statistically analyzed. The experiment was repeated three times with the same results.

pathogenicity of Δ*Mohat1*:MoHAT1^{DTB} strain was similar to the wild type (Fig. 6C, D). Accordingly, a lesion-type scoring assay (Wang et al., 2013) confirmed that most of the lesions caused by milR236-OE and Δ*Mohat1* mutants were of types 1–3 with very few being type 4. There were no severe type 5 lesions found (Fig. 6D).

By observing appressorium formation on the artificial inductive surfaces, we found that milR236-OE exhibited delayed appressorium differentiation, similar to that of the Δ*Mohat1* mutant when compared with the wild-type strain. But the appressorium differentiation of milR236-OE/MoHAT1^{DTB} strain was similar to that of Guy11. The percentage of appressorium formation was significantly lower in the milR236-OE and Δ*Mohat1* mutants at 2–8 hpi, but the difference became less distinguishable after 10 hpi (Fig. 6E). This suggested that appressorium formation is also regulated by milR236 and *MoHAT*^{DTB} interferes with milR236 on *MoHAT1*.

To understand the mechanism underlying the reduced virulence, the appressorium turgor was measured. We found that the collapse rates in the presence of 1, 2, 3, and 4 M glycerol were higher in the milR236-OE and Δ*Mohat1* mutant (Fig. 6F), indicating that milR236 influences appressorium turgor generation. We then performed a host penetration assay using detached rice sheaths using the previously reported methods (Chen et al., 2014; Qi et al., 2016) and found that, at 48 hpi, the invasive hyphae (IH) of Guy11, milR236-OE:MoHAT1^{DTB} and Δ*Mohat1*:MoHAT1^{DTB} strain spread to the adjacent cells, whereas the IH of the Δ*Mohat1* mutant and milR236-OE were limited to one cell (Fig. 6G). Taken together, these findings suggested that milR236 is important for IH growth.

4. Discussion

The rice blast fungus *M. oryzae* evolves multifaceted regulatory mechanisms, including G proteins and RGS proteins, to govern its growth, differentiation, and pathogenicity (Zhang et al., 2011b). We hypothesized that the important roles of *M.* oryzae RGS proteins may involve the regulatory functions of sRNAs and profiled their expression. Using sRNA-Seq analysis, we identified 219 milRNAs at 4 hpi correlating to the appressorium development stage and found out that the expression of sRNA, especially milRNA, was impacted by the disruptions of genes encoding RGS proteins. By analyzing one of the differentially expressed milRNAs, milR236, we demonstrated that the milRRNA regulates MoHat1 expression while itself is subject to regulation by the transcription factor MoMsn2. These multifaceted regulatory mechanisms collectively govern appressorium formation and virulence of the blast fungus.

Previous studies have demonstrated that sRNAs are involved in the developmental processes of *M. oryzae*, including growth, appressorium development, and virulence (Raman et al., 2017). Various physiological stressors alter the transcriptional levels of sRNAs, and the characteristics of sRNAs may also differ during the different developmental stages (Nunes et al., 2011; Raman et al., 2013). Intriguingly, no conventional miRNAs but only milRNAs were present in *M. oryzae.* This is similar to a study in *N. crassa* (Lee et al., 2010). Similar findings were also reported for the white mold fungus *Sclerotinia sclerotiorum* (Zhou et al., 2012) and the wilt fungus *V. dahliae* (Jin et al., 2019). Either the accumulation of miRNAs was less abundant, the expression was transient, or only milRNAs in fungi are all possible scenarios for fungi not having miRNAs. Regardless, evidence suggested that milRNAs are a group of conserved regulators for gene expression in fungi (Chen et al., 2015; Lee et al., 2010).

The architecture of transcription factor binding motifs may be conserved in miRNAs that respond to particular stressors (Devi et al., 2013). Similar mechanisms may also exist for milRNAs in *M. oryzae.* Here, 121 DE-milRNA promoter regions contained the putative motifs were predicted using MEME (Fig. 1B, Table S3), and it reached to 70.76% of total DE-milRNAs. This predicted binding motif was conserved in these milRNAs that responded to MoRGS mutants at 4 hpi. The binding motif of MoMsn2, sharing the highest similarity to the predicted motif, may play an important role in the regulation of milRNAs present in MoRGS mutants.

As stated previously, miRNAs play critical roles in the regulation of

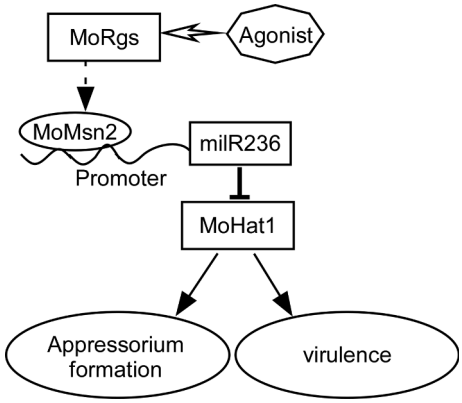

Fig. 7. A proposed model of MoRGS and milRNA regulating appressorium formation and virulence. MoRGS positively regulates the expression of the transcription factor MoMsn2 while it regulates the expression of milR236 by binding to the promoter of milR236. milR236 suppresses the transcription of *MoHAT1*. The deletion of the *MoHAT1* gene results in delayed appressorium formation and attenuated virulence. The milR236-overexpression (milR236-OE) strain shares similar defects as the Δ*Mohat1* mutant strain. MoMsn2 binds to the promoter of milR236 to regulate its expression, further suppressing *MoHAT1* transcription to regulate appressorium formation and virulence in *M. oryzae*.

cellular growth and development by regulating the expression of target genes through RNA cleavage or transcriptional silencing at both transcriptional and post-transcriptional levels (He and Hannon, 2004). In rice, miR169 (Osa-miR169) represses the transcription of the NF-YA family target genes with the exception of *Os03g29760/NF-YA2*, but miR169a can regulate the expression of *Os03g29760* via translation inhibition (Li et al., 2017). Here, we examined the target gene expression only at the transcriptional level but not translation. Nevertheless, our data have shown that milR236 represses the transcription of *MoHAT1* at several developmental stages. In addition, co-expression of milR236 and MoHat1 downregulate the accumulation of MoHat1 significantly lower than those through the co-expression of milR236 and target mimicry MoHat1^{DTB}.

In summary, we proposed a model of a regulatory mechanism underlying the function of milR236 during appressorium formation and plant infection by *M. oryzae* (Fig. 7). Surface cues sensed by *M. oryzae* MoRGS mutations positively regulate the downstream networks, in conjunction with the transcription factor MoMsn2 that binds to the promoter of milR236. The resulting regulation, in turn, suppresses the expression of the *MoHAT1* target gene, resulting in a delay in appressorium formation and attenuation in virulence. Our studies shed new light on multifaceted regulatory pathways that govern the appressorium formation and virulence of *M. oryzae*.

Acknowledgments

Funding: This research was supported by the key program of the Natural Science Foundation of China (Grant No: 31530063, ZZ), Natural Science Foundation of China (Grant No: 31470248, XZ), and Innovation Team Program for Jiangsu Universities (2017). The Wang laboratory research was partially supported by NIH grant AI149289 (USA). We thank Prof. Hongwei Zhao (Nanjing Agricultural University, Nanjing) for stimulating discussion and Zhaoyun Wang and Yeqiang Xia for technique assistance.

Appendix A. Supplementary material

Supplementary data to this article can be found online at https://doi.org/10.1016/j.fgb.2020.103349.

References

Chen, Y., Gao, Q., Huang, M., Liu, Y., Liu, Z., Liu, X., Ma, Z., 2015. Characterization of RNA silencing components in the plant pathogenic fungus *Fusarium graminearum*. Sci. Rep. 5, 12500.
Chen, Y., Zuo, R.F., Zhu, Q., Sun, Y., Li, M.Y., Dong, Y.H., Ru, Y.Y., Zhang, H.F., Zheng, X.B., Zhang, Z.G., 2014. MoLys2 is necessary for growth, conidiogenesis, lysine biosynthesis, and pathogenicity in *Magnaporthe oryzae*. Fung. Genet. Biol. 67, 51–57.
De Vries, L., Zheng, B., Fischer, T., Elenko, E., Farquhar, M.G., 2000. The regulator of G protein signaling family. Annu. Rev. Pharmacol. Toxicol. 40, 235–271.
Devi, S.J., Madhav, M.S., Kumar, G.R., Goel, A.K., Umakanth, B., Jahnavi, B., Viraktamath, B.C., 2013. Identification of abiotic stress miRNA transcription factor binding motifs (TFBMs) in rice. Gene 531, 15–22.
Dohlman, H.G., Thorner, J.W., 2001. Regulation of G protein-initiated signal transduction in yeast: paradigms and principles. Annu. Rev. Biochem. 70, 703–754.
Dong, Y., Li, Y., Zhao, M., Jing, M., Liu, X., Liu, M., Guo, X., Zhang, X., Chen, Y., Liu, Y., et al., 2015. Global genome and transcriptome analyses of *Magnaporthe oryzae* epidemic isolate 98–06 uncover novel effectors and pathogenicity-related genes, revealing gene gain and lose dynamics in genome evolution. PLoS Pathog. 11, e1004801.
Gowda, M., Nunes, C.C., Sailsbery, J., Xue, M., Chen, F., Nelson, C.A., Brown, D.E., Oh, Y., Meng, S., Mitchell, T., et al., 2010. Genome-wide characterization of methylguanosine-capped and polyadenylated small RNAs in the rice blast fungus *Magnaporthe oryzae*. Nucl. Acids Res. 38, 7558–7569.
Guo, A.Y., Sun, J., Jia, P., Zhao, Z., 2010. A novel microRNA and transcription factor mediated regulatory network in *schizophrenia*. BMC Syst. Biol. 4, 10.
Hackenberg, M., Shi, B.J., Gustafson, P., Langridge, P., 2012. A transgenic transcription factor (TaDREB3) in barley affects the expression of microRNAs and other small non-coding RNAs. PLoS ONE 7, e42030.
He, L., Hannon, G.J., 2004. MicroRNAs: small RNAs with a big role in gene regulation. Nat. Rev. Genet. 5, 522–531.
Hu, J., Zhu, Y., 2017. Nonradioactive plant small RNA detection using biotin-labeled probes. Methods Mol. Biol. 1640, 211–217.
Huang, Q., Mao, Z., Li, S., Hu, J., Zhu, Y., 2014. A non-radioactive method for small RNA detection by northern blotting. Rice (N Y) 7, 26.
Jin, Y., Zhao, J.H., Zhao, P., Zhang, T., Wang, S., Guo, H.S., 2019. A fungal milRNA mediates epigenetic repression of a virulence gene in *Verticillium dahliae*. Philos. Trans. R. Soc. Lond. B Biol. Sci. 374, 20180309.
Kadotani, N., Nakayashiki, H., Tosa, Y., Mayama, S., 2003. RNA silencing in the phytopathogenic fungus *Magnaporthe oryzae*. Mol. Plant-Microbe Interact.: MPMI 16, 769–776.
Lee, H.C., Li, L., Gu, W., Xue, Z., Crosthwaite, S.K., Pertsemlidis, A., Lewis, Z.A., Freitag, M., Selker, E.U., Mello, C.C., et al., 2010. Diverse pathways generate microRNA-like RNAs and Dicer-independent small interfering RNAs in fungi. Mol. Cell 38, 803–814.
Li, Y., Zhang, Z., Liu, F., Vongsangnak, W., Jing, Q., Shen, B., 2012. Performance comparison and evaluation of software tools for microRNA deep-sequencing data analysis. Nucl. Acids Res. 40, 4298–4305.
Li, Y., Zhao, S.L., Li, J.L., Hu, X.H., Wang, H., Cao, X.L., Xu, Y.J., Zhao, Z.X., Xiao, Z.Y., Yang, N., et al., 2017. Osa-miR169 negatively regulates rice immunity against the blast fungus *Magnaporthe oryzae*. Front. Plant Sci. 8, 2.
Nakayashiki, H., 2005. RNA silencing in fungi: mechanisms and applications. FEBS Lett. 579, 5950–5957.
Nunes, C.C., Gowda, M., Sailsbery, J., Xue, M., Chen, F., Brown, D.E., Oh, Y., Mitchell, T.K., Dean, R.A., 2011. Diverse and tissue-enriched small RNAs in the plant pathogenic fungus, *Magnaporthe oryzae*. Bmc Genom. 12, 288.
Qi, Z.Q., Liu, M.X., Dong, Y.H., Zhu, Q., Li, L.W., Li, B., Yang, J., Li, Y., Ru, Y.Y., Zhang, H.F., et al., 2016. The syntaxin protein (MoSyn8) mediates intracellular trafficking to regulate conidiogenesis and pathogenicity of rice blast fungus. New Phytol. 209, 1655–1667.
Qin, S., Parthun, M.R., 2002. Histone H3 and the histone acetyltransferase Hat1p contribute to DNA double-strand break repair. Mol. Cell. Biol. 22, 8353–8365.
Raman, V., Simon, S.A., Demirci, F., Nakano, M., Meyers, B.C., Donofrio, N.M., 2017. Small RNA functions are required for growth and development of *Magnaporthe oryzae*. Mol. Plant-Microbe Interact.: MPMI 30, 517–530.
Raman, V., Simon, S.A., Romag, A., Demirci, F., Mathioni, S.M., Zhai, J., Meyers, B.C., Donofrio, N.M., 2013. Physiological stressors and invasive plant infections alter the small RNA transcriptome of the rice blast fungus, *Magnaporthe oryzae*. Bmc Genom. 14, 326.
Ruby, J.G., Jan, C., Player, C., Axtell, M.J., Lee, W., Nusbaum, C., Ge, H., Bartel, D.P., 2006. Large-scale sequencing reveals 21U-RNAs and additional microRNAs and endogenous siRNAs in C. elegans. Cell 127, 1193–1207.
Schwab, R., Ossowski, S., Riester, M., Warthmann, N., Weigel, D., 2006. Highly specific gene silencing by artificial microRNAs in *Arabidopsis*. Plant Cell 18, 1121–1133.
Varkonyi-Gasic, E., Wu, R., Wood, M., Walton, E.F., Hellens, R.P., 2007. Protocol: a highly sensitive RT-PCR method for detection and quantification of microRNAs. Plant Methods 3, 12.
Wang, J., Yin, Z., Tang, W., Cai, X., Gao, C., Zhang, H., Zheng, X., Wang, P., Zhang, Z., 2017. The thioredoxin MoTrx2 protein mediates reactive oxygen species (ROS) balance and controls pathogenicity as a target of the transcription factor MoAP1 in *Magnaporthe oryzae*. Mol. Plant Pathol 18, 1199–1209.
Wang, J.M., Du, Y., Zhang, H.F., Zhou, C., Qi, Z.Q., Zheng, X.B., Wang, P., Zhang, Z.G., 2013. The actin-regulating kinase homologue MoArk1 plays a pleiotropic function in *Magnaporthe oryzae*. Mol. Plant Pathol. 14, 470–482.
Yin, Z., Chen, C., Yang, J., Feng, W., Liu, X., Zuo, R., Wang, J., Yang, L., Zhong, K., Gao, C., et al., 2019. Histone acetyltransferase MoHat1 acetylates autophagy-related

proteins MoAtg3 and MoAtg9 to orchestrate functional appressorium formation and pathogenicity in *Magnaporthe oryzae*. Autophagy 1–24.
Zhang, C., Wang, G., Wang, J., Ji, Z., Liu, Z., Pi, X., Chen, C., 2013. Characterization and comparative analyses of muscle transcriptomes in *Dorper* and small-tailed Han sheep using RNA-Seq technique. PLoS ONE 8, e72686.
Zhang, H., Liu, K., Zhang, X., Tang, W., Wang, J., Guo, M., Zhao, Q., Zheng, X., Wang, P., Zhang, Z., 2011a. Two phosphodiesterase genes, PDEL and PDEH, regulate development and pathogenicity by modulating intracellular cyclic AMP levels in *Magnaporthe oryzae*. PLoS ONE 6, e17241.
Zhang, H., Zhao, Q., Guo, X., Guo, M., Qi, Z., Tang, W., Dong, Y., Ye, W., Zheng, X., Wang, P., et al., 2014. Pleiotropic function of the putative zinc-finger protein MoMsn2 in *Magnaporthe oryzae*. Mol. Plant-Microbe Interact.: MPMI 27, 446–460.
Zhang, H.F., Tang, W., Liu, K.Y., Huang, Q., Zhang, X., Yan, X., Chen, Y., Wang, J.S., Qi, Z. Q., Wang, Z.Y., et al., 2011b. Eight RGS and RGS-like proteins orchestrate growth, differentiation, and pathogenicity of Magnaporthe oryzae. PLoS pathogens 7.
Zhang, S.L., Liang, M.L., Naqvi, N.I., Lin, C.X., Qian, W.Q., Zhang, L.H., Deng, Y.Z., 2017. Phototrophy and starvation-based induction of autophagy upon removal of Gcn5-catalyzed acetylation of Atg7 in *Magnaporthe oryzae*. Autophagy 13, 1318–1330.
Zhou, J., Fu, Y., Xie, J., Li, B., Jiang, D., Li, G., Cheng, J., 2012. Identification of microRNA-like RNAs in a plant pathogenic fungus *Sclerotinia sclerotiorum* by high-throughput sequencing. Mol. Genet. Genom.: MGG 287, 275–282.